

## The Low Lying Electronic States of Dichloromaleic Anhydride

Yoshimi ISHIBASHI, Ryoichi SHIMADA,<sup>†</sup> and Hiroko SHIMADA\*

Department of Chemistry, Faculty of Science, Fukuoka University,  
Nanakuma, Jonan-ku, Fukuoka 814

<sup>†</sup> Department of Chemistry, Faculty of Science, Kyushu University 33,  
Hakozaki, Higashi-ku, Fukuoka 812

(Received December 18, 1982)

The polarized Raman and infrared spectra of dichloromaleic anhydride were studied and the assignments of the normal vibrations were reinvestigated based on the polarization behaviors of the spectral bands and on the normal coordinate calculation. Using the assignments the vibrational structure of the phosphorescence spectrum was analyzed and the phosphorescence lifetime was also measured. These results indicate that the lowest triplet state of this molecule is a  $^3(\pi, \pi^*)$  state perturbed by closely located  $^3(n, \pi^*)$  states. The near ultraviolet absorption and phosphorescence excitation spectra were measured and four absorption bands due to  $^3(n, \pi^*) \leftarrow ^1A_1$ ,  $^1A_2(n, \pi^*) \leftarrow ^1A_1$ ,  $^1B_1(n, \pi^*) \leftarrow ^1A_1$ , and  $^1A_1(\pi, \pi^*) \leftarrow ^1A_1$  transitions were found. The polarization experiment made on the  $^1A_2(n, \pi^*) \leftarrow ^1A_1$  absorption suggests that this transition borrows the intensity from the  $^1A_1(\pi, \pi^*) \leftarrow ^1A_1$  transition.

The assignments of the normal vibrations of dichloromaleic anhydride were first made by Rogstad *et al.*<sup>1)</sup> based on the infrared vapor contours, the depolarization measurement of the Raman bands and the normal coordinate calculation. Their assignments given for the non-totally symmetric vibrations seem to be unreliable because the assignments were not made based on the enough experimental evidences and the reasonable vibrational analysis of the phosphorescence spectrum could not be made using their assignments.

The near ultraviolet absorption spectra and phosphorescence lifetimes of maleic anhydride and its halo derivatives were first studied by Scharf and Leismann.<sup>2)</sup> They suggested that the lowest singlet and triplet states of dichloromaleic anhydride are to be a  $^1(n, \pi^*)$  and a mixed state of  $^3(n, \pi^*)$  and  $^3(\pi, \pi^*)$  configurations, respectively. Detailed studies for the electronic states of these molecules have not been made yet.

In this work, the assignments of the normal vibrations of dichloromaleic anhydride are reexamined on the basis of the polarization behaviors of the Raman and infrared spectra and the assignments given for several bands by previous workers are corrected. The low lying excited singlet and triplet states of this molecule are studied in detail through the vibrational analyses of the phosphorescence and phosphorescence excitation spectra and also the polarized near ultraviolet absorption spectrum.

### Experimental

**Material.** Dichloromaleic anhydride obtained from Aldrich Company was purified by zone-refining of about 100 passages followed by sublimation under reduced pressure. Cyclohexane of Dotite Spectrosol grade was purified by passing through the activated silica gel and alumina columns.

**Optical Measurement.** The Raman spectrum was observed in the liquid and single crystal phases with a JEOL 400 T Laser Raman Spectrophotometer. The sample was excited with the 514.5 nm beam from an Ar<sup>+</sup> ion laser. The single crystal was obtained in the following way. The sample was sealed in a evacuated closed glass tube. Temperature of one side of the tube, where the sample was placed, was kept a little higher than the other side. Crystals grown in the tube were collected. The well grown and approximately rectangular shaped single crystal was selected with a polarization

microscope and used for the observation of the polarized Raman spectrum. Although the crystal structure of dichloromaleic anhydride was not determined yet, the directions of the crystal growth and the two-fold symmetry axis of the crystal were found to be the crystal axes by observation of the birefringence under the polarization microscope. These axes were tentatively taken to be the c and b axes, respectively. The a axis was taken to be perpendicular to both the b and c axes. The method of the measurement of the polarized Raman spectrum was exactly the same as that described previously.<sup>3)</sup>

The infrared spectrum was observed with a Hitachi Infrared Spectrophotometer Model 345 over the range of 4000–250 cm<sup>-1</sup> in the vapor and single crystal phases. The vapor spectrum was observed at 50 °C with a gas cell of 10 cm in optical path. The polarized infrared spectrum of a single crystal grown between two KRS-5 plates was measured with an AgBr wire-grid polarizer by the method described in the previous paper.<sup>4)</sup> The infrared spectrum of the thin film obtained by sublimation was also observed.

The phosphorescence lifetime and the time resolved phosphorescence spectrum were measured in cyclohexane at 1.4 K using the optical setup described in the previous paper.<sup>5)</sup> The short lifetime phosphorescence was observed in the following way. The sample was excited for 40 ms and the excitation was cut off. 1 ms after ceasing the excitation, the phosphorescence was sampled for 40 ms. The longer lifetime phosphorescence was observed with the exciting, waiting and sampling times of 120, 360, and 120 ms, respectively.

The excitation spectrum was observed in cyclohexane at 77 K monitoring the intensity of the phosphorescence 0–0 band with the excitation light source of a 500 W Xenon arc lamp of Ushio UXL-500D. The near ultraviolet absorption spectrum was observed in cyclohexane and in the thin film at room temperature and at 77 K with a Hitachi Ultraviolet Spectrophotometer Model 323 over the range of 500–210 nm. The polarized ultraviolet absorption spectrum was also measured with the single crystal grown between two quartz plates over the range of 350–315 nm.

### Normal Coordinate Calculation

A normal coordinate calculation was performed through the standard GF matrix method with FACOM M-200 computer at the computer center of Kyushu University. Hilderbrandt *et al.*<sup>6)</sup> showed that the mo-

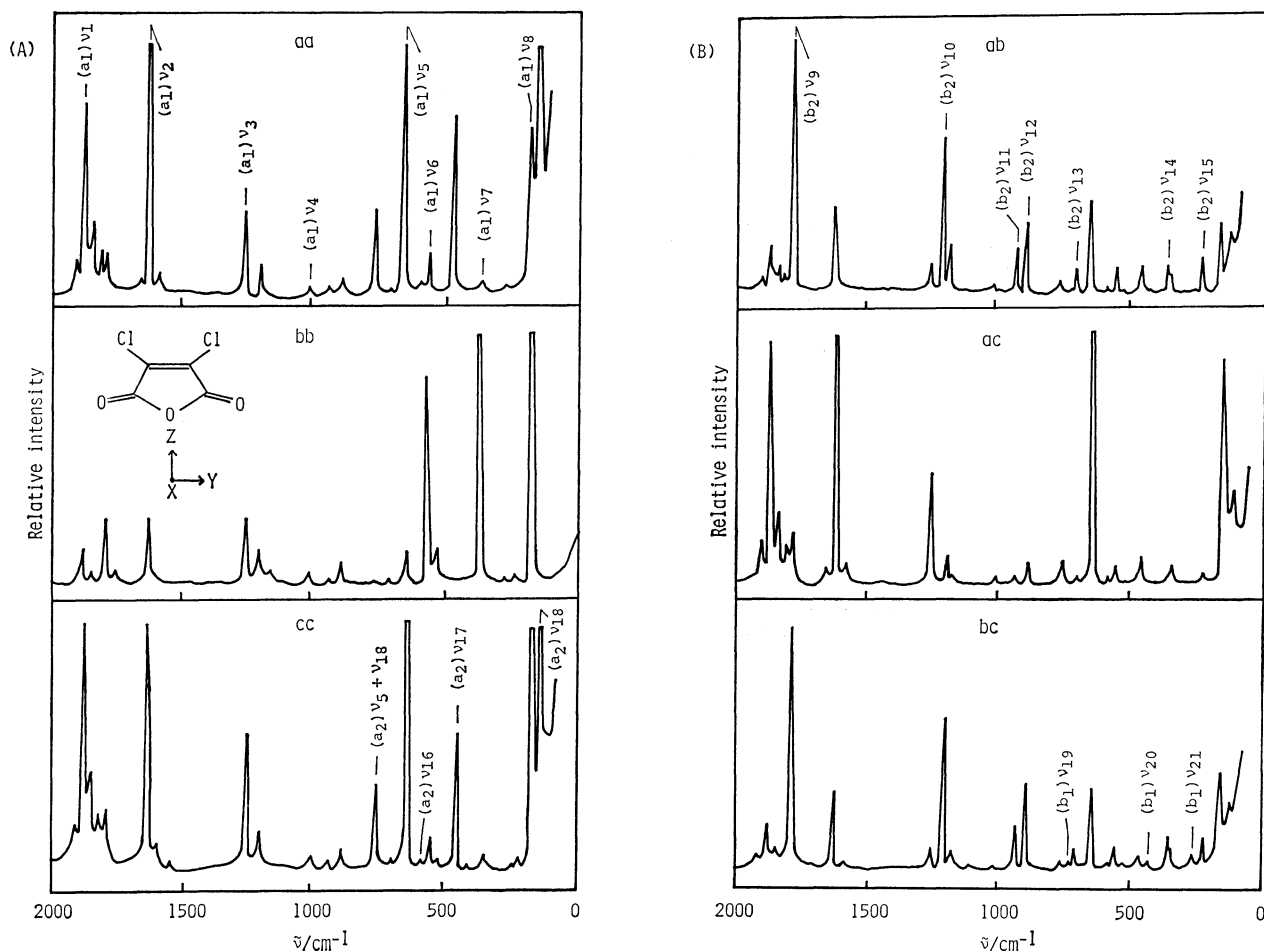


Fig. 1. Polarized Raman spectrum of the dichloromaleic anhydride single crystal. (A): aa, bb, and cc spectra, (B): ab, ac, and bc spectra.

TABLE 1. FORCE CONSTANTS FOR THE IN-PLANE VIBRATIONS OF DICHLOROMALEIC ANHYDRIDE

$K_{C'-C'}$	8.15	$F_{C' \cdots Cl}$	0.65
$K_{C'-C}$	3.52	$F_{C \cdots Cl}$	0.63
$K_{C-O'}$	2.60	$F_{C' \cdots O}$	0.30
$K_{C'-Cl}$	3.20	$F_{O' \cdots O}$	0.54
$K_{C=O}$	10.83	$k_{Cl, r_{Cl}}^o$	0.08
$H_{C'-C'-C}$	0.03	$k_{Cl, r_{O}}^o$	0.03
$H_{C'-C-O'}$	0.49	$k_{O, r_{O}}^m$	0.08
$H_{C-O'-C}$	0.50	$k_{R, R}^m$	-0.02
$H_{C'-C'-Cl}$	0.07	$h_{R, \alpha_O}^m$	0.03
$H_{C'-C-Cl}$	0.10	$h_{R, \alpha_C}^m$	0.01
$H_{C'-C=O}$	0.28	$h_{R, \beta_O}^m$	-0.02
$H_{O'-C=O}$	0.65	$h_{R, \beta_{Cl}}^m$	-0.01
$F_{C \cdots C'}$	0.60	$f_{\alpha, \alpha}^o$	0.03
$F_{C' \cdots O'}$	0.74	$f_{\beta_{Cl}, \beta_O}^o$	0.05
$F_{C \cdots C}$	0.96	$f_{\beta_{Cl}, \beta_{Cl}}^o$	0.01

Force constants denoted by  $K$ ,  $H$ ,  $F$ , and  $k$  are given in  $\text{J/dm}^2$  ( $=\text{mdyn/\AA}$ ) units, and those denoted by  $h$  and  $f$  are in  $\text{pJ/dm rad}$  ( $=\text{mdyn/rad}$ ) and  $\text{aJ/rad}^2$  ( $=\text{mdyn \AA/rad}^2$ ) units, respectively.  $C'$  is the carbon atom bonded to  $Cl$ .  $O'$  is the oxygen atom in the ring.

TABLE 2. FORCE CONSTANTS FOR THE OUT-OF-PLANE VIBRATIONS OF DICHLOROMALEIC ANHYDRIDE

$Q_{C=C}$	0.35	$p_{Cl, Cl}^o$	0.04
$Q_{C-C}$	0.70	$p_{Cl, O}^o$	0.03
$Q_{C-O}$	0.80	$p_{O, O}^m$	0.03
$q_{C=C, C-C}^o$	-0.05	$p_{Cl, O}^m$	0.01
$q_{C=C, C-O}^o$	-0.08	$t_{C=C, Cl}^o$	-0.12
$q_{C=C, O-C}^o$	-0.03	$t_{C-O, O}^o$	-0.10
$q^m$	0.02	$t_{C-O, O}^o$	-0.06
$P_{Cl}$	0.36	$t_{C-O, Cl}^o$	-0.04
$P_O$	0.34		

Force constants are given in  $\text{aJ/rad}^2$  ( $=\text{mdyn \AA/rad}^2$ ) units.

molecular structure of maleic anhydride belongs to the point group  $C_{2v}$  and gave the geometric parameters for the molecular structure. We assumed that the molecular geometry of dichloromaleic anhydride was the same as that of maleic anhydride except for the  $C-Cl$  bond, whose distance was assumed to be 0.177 nm.

The  $F$  matrix elements for the in-plane and out-of-plane vibrations were evaluated with the potential fields of an improved modification of the Urey-Bradley force field and the valence force field, respectively, as used for the calculation made on maleic anhydride.<sup>9)</sup>

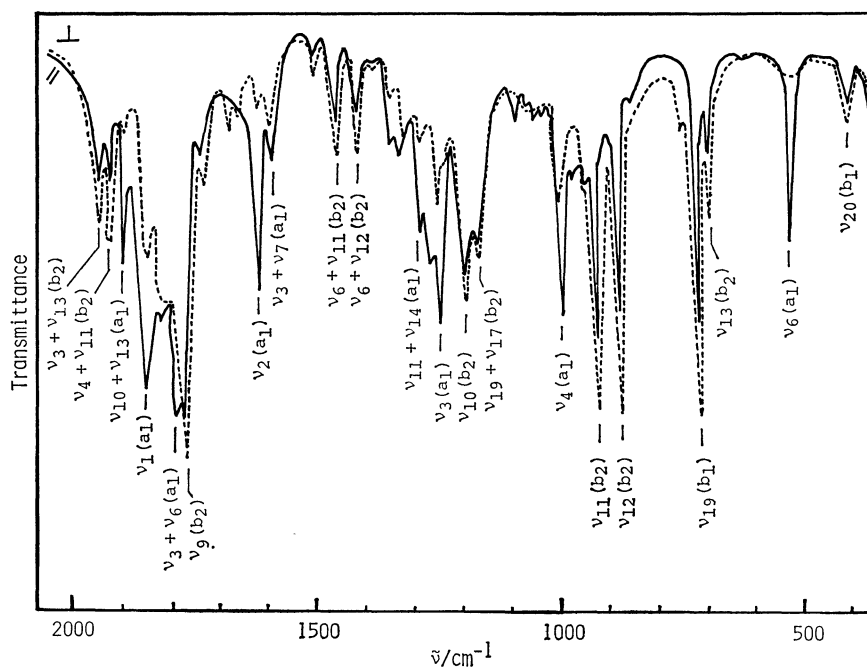


Fig. 2. Polarized infrared spectrum of the dichloromaleic anhydride single crystal.

The notations of the force constants are exactly the same as those given in the previous calculation.<sup>3)</sup>

### Results and Discussion

**Normal Vibration.** The force constants finally obtained after several iterative normal coordinate calculations for the in-plane and out-of-plane vibrations are given in Tables 1 and 2, respectively. The calculated frequencies and vibrational modes are given in Table 3, together with the experimentally assigned vibrational frequencies.

The polarized Raman spectrum is shown in Fig. 1. The spectrum was denoted by two symbols such as *ab*. The first letter refers to the direction of the polarization of the excitation light and the second to that of the scattering light. The non-totally symmetric Raman bands were divided into three types of polarization behavior according to the relative intensities of the bands in the polarized spectrum. The intensities of the bands belonging to the first type are much stronger in the *ab* and *bc* spectra than those in other spectra. The intensities of the second type bands are much stronger in the *aa* and *cc* spectra than those in other spectra, and the third type bands can be observed only in the *bc* spectrum with appreciable intensity.

The polarized infrared spectrum observed in the single crystal is shown in Fig. 2. The spectra measured with the incident lights polarized parallel and perpendicular to the crystal growth direction are referred to as *//* and *⊥* spectra and drawn with the solid and dotted lines, respectively. The polarized infrared bands can be divided into two types according to their polarization behaviors. The bands belonging to the first type appear strongly in the *//* spectrum and extremely weakly in the *⊥* spectrum. The bands

belonging to the second type appear strongly in the *⊥* spectrum and weakly in the *//* spectrum. These two types of the bands are denoted as types I and II, respectively. Rogstad *et al.*<sup>4)</sup> indicated that the infrared vapor bands belonging to the *a*<sub>1</sub>, *b*<sub>1</sub>, and *b*<sub>2</sub> symmetry species show the B, C, and A band envelopes, respectively, from the calculated values of the moments of inertia, where the *z* axis was taken to be along the C<sub>2</sub> symmetry axis and the *x* axis to be perpendicular to the molecular plane.

The assignments of the normal vibrations belonging to each symmetry species were made based on the following observations.

***a*<sub>1</sub> Species:** The polarized bands in the depolarization measurement of the Raman spectrum can be definitely assigned to the *a*<sub>1</sub> vibrations. The infrared crystal bands showing the type I polarization behavior are also to be assigned to the *a*<sub>1</sub> bands, since the corresponding infrared vapor bands showed the B band envelope and the frequencies coincide with those of the Raman *a*<sub>1</sub> bands.

***b*<sub>2</sub> Species:** The *b*<sub>2</sub> bands showing the A band envelope in the infrared vapor spectrum showed the type II polarization behavior in the infrared crystal spectrum. The corresponding Raman bands were observed strongly in the *ab* and *bc* polarized Raman spectra.

***b*<sub>1</sub> Species:** The *b*<sub>1</sub> bands showing the C band envelope in the infrared vapor spectrum showed the type II polarization behavior in the infrared crystal spectrum. The corresponding Raman bands were observed only in the *bc* polarized Raman spectrum with appreciable intensity.

***a*<sub>2</sub> Species:** The crystal Raman bands showing the *aa* and *cc* polarization behavior should be assigned to the *a*<sub>2</sub> vibration, because other two polarization behaviors of the Raman bands were already ascribed

TABLE 3. NORMAL VIBRATIONS OF DICHLOROMALEIC ANHYDRIDE

Sym. species	Vibrational mode	Raman			Infrared			Calcd $\bar{\nu}/\text{cm}^{-1}$	Obsd Rogstad <i>et al.</i> $\bar{\nu}/\text{cm}^{-1}$
		Liquid		Crystal Pol.	Crystal		Vapor type		
		$\bar{\nu}/\text{cm}^{-1}$	Pol.		$\bar{\nu}/\text{cm}^{-1}$	Pol.			
a <sub>1</sub>	$\nu_1$ C=O str.	1868	p		1858	I		1869	1870
	$\nu_2$ C=C str.	1616	p		1613	I	B	1619	1623
	$\nu_3$ C-O str.	1245	p		1245	I	B	1246	1244
	$\nu_4$ C-C str.	1003	p		1007	I	B	1006	1003
	$\nu_5$ Ring def.	640	p					642	637
	$\nu_6$ C-Cl str.	545	p		542	I	B	538	540
	$\nu_7$ C=O bend.	351	p					352	350
	$\nu_8$ Cl bend.	175	p?					153	188
b <sub>2</sub>	$\nu_9$ C=O str.	1792	dp	ab, bc	1780	II	A	1793	1799
	$\nu_{10}$ C-C str.	1203	dp	ab, bc	1200	II	A	1206	1201
	$\nu_{11}$ C-O str.	932	dp	ab, bc	916	II	A	934	926
	$\nu_{12}$ C-Cl str.	884	dp	ab, bc	872	II	A	886	884
	$\nu_{13}$ C=O bend.	697	dp	ab, bc	697	II	A	698	697
	$\nu_{14}$ Ring def.	356	dp	ab, bc				356	419
	$\nu_{15}$ Cl bend.	237	dp	ab, bc				239	174
	a <sub>2</sub>	$\nu_{16}$ Ring def.	585	dp	aa, cc				585
$\nu_{17}$ C=O wag.		463	dp	aa, cc				468	462
$\nu_{18}$ Cl wag.		123	dp	aa, cc				132	127
b <sub>1</sub>	$\nu_{19}$ Ring def.	723		bc	718	II	C	719	723
	$\nu_{20}$ C=O wag.	421	dp	bc	419	II	C	420	258
	$\nu_{21}$ Cl wag.	255		bc				238	236

to the  $b_2$  and  $b_1$  vibrations, and no corresponding bands were observed in the infrared spectrum.

The normal vibration thus determined are given in Table 3 and also shown in Figs. 1 and 2. The assignments for the  $a_1$  vibrations given in this work exactly agree with those given by Rogstad *et al.*<sup>1)</sup> This is quite natural because the  $a_1$  vibrations were straightforwardly determined based on the depolarization measurement of the Raman bands. On the other hand, our assignments given for the non-totally symmetric vibrations were somewhat different from those given by them as can be seen in Table 3. Rogstad *et al.*<sup>1)</sup> gave the assignments based on the band envelope in the infrared vapor spectrum, where only four band envelopes could be observed. In our work, the assignments were made based on the polarization behaviors of the Raman and infrared bands and also on the band envelope in the infrared vapor spectrum, where eleven band envelopes were observed. Therefore, we believe that our assignments are to be more reliable than those given by Rogstad *et al.*

**Phosphorescence Spectrum.** Dichloromaleic anhydride emits a weak yellow phosphorescence in cyclohexane matrix. Scharf and Leismann<sup>2)</sup> measured the phosphorescence lifetime in mixed solvents of methylcyclohexane and isopentane, and of ethanol and isopentane at 77 K and got the lifetimes of 13.9 and 75 ms, respectively. We analyzed the phosphorescence decays observed in cyclohexane at 1.4 K with changing the exciting, waiting and sampling times of the phosphorescence and obtained the lifetimes of 62 and about 300 ms. The third lifetime component could

not be precisely measured due to its extremely weak intensity. The decay analysis showed that the third lifetime is longer than 1500 ms. These values of the lifetime would be reasonable because the lifetime observed in cyclohexane at 77 K was 150 ms. We also traced the measurement made by Scharf and Leismann, but we could not reproduce their results.

The time resolved phosphorescence spectrum is shown in Fig. 3. The vibrational analysis of the short lifetime phosphorescence spectrum will be discussed first. The strongest and shortest wavelength band observed at 477.88 nm was taken as the 0-0 band. Very strong bands separated by 639 and 1621  $\text{cm}^{-1}$  from the 0-0 band were assigned to the ring deformation ( $\nu_5$ ) and C=C stretching ( $\nu_2$ ) vibrations, respectively. These bands constitute the main progressions. Medium intense bands separated by 180, 1008, 1245, and 1881  $\text{cm}^{-1}$  from the 0-0 band were assigned to the Cl bending ( $\nu_8$ ), C-C stretching ( $\nu_4$ ), and C-O stretching ( $\nu_3$ ), and C=O stretching ( $\nu_1$ ) vibrations, respectively. These bands belong to the totally symmetric species. A medium intense band separated by 420  $\text{cm}^{-1}$  from the 0-0 band was assigned to the C=O wagging ( $\nu_{20}$ ) vibration of the  $b_1$  symmetry species. Medium intense bands separated by 453 and 585  $\text{cm}^{-1}$  were assigned to the C=O wagging ( $\nu_{17}$ ) and ring deformation ( $\nu_{16}$ ) vibrations of the  $a_2$  species, respectively. Detailed vibrational analysis is given in Fig. 3.

The middle lifetime phosphorescence spectrum could not be successfully measured because of its very weak intensity. The intensity ratio of the 0-0 bands of the middle and short lifetime phosphorescence spectra was

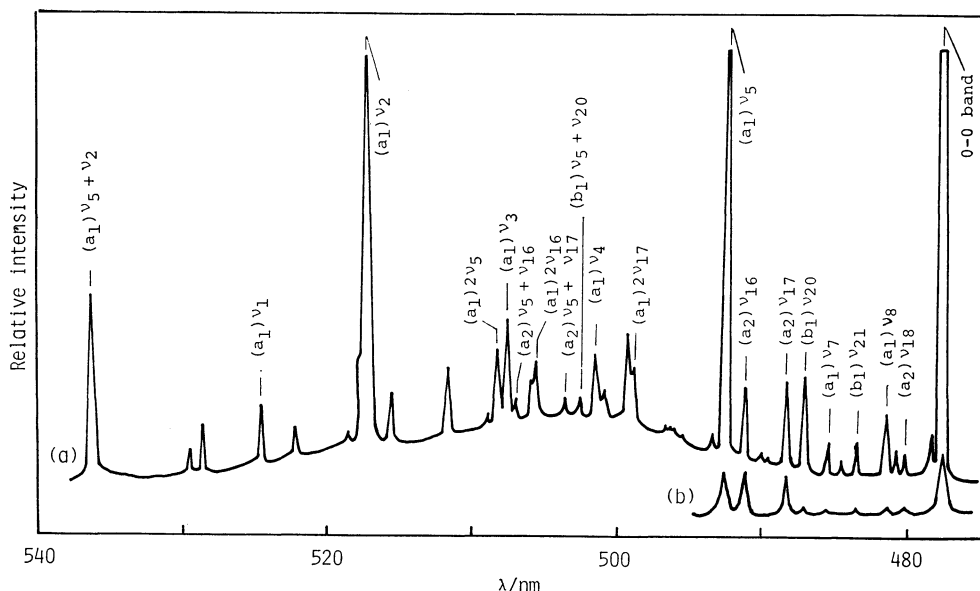


Fig. 3. Phosphorescence spectrum of dichloromaleic anhydride in cyclohexane at 1.4 K. The exciting, waiting, and sampling times of the phosphorescence are (a): 40, 1, 40 ms, (b): 120, 360, and 120 ms, respectively.

measured to be less than 1/100. The most characteristic spectral feature of the middle lifetime phosphorescence is that the relative intensities of the bands assigned to the Cl wagging ( $\nu_{18}$ ), C=O wagging ( $\nu_{17}$ ), and ring deformation ( $\nu_{16}$ ) vibrations of the  $a_2$  species to the intensity of the 0-0 band remarkably increased compared with those of the short lifetime phosphorescence.

A weak phosphorescence excitation spectrum was observed in the 450 nm region in cyclohexane at 77 K, but no spectrum could be observed in the 470 nm region. A extremely weak absorption spectrum was also observed in the 450 nm region with the  $f$ -value of about  $1 \times 10^{-7}$  in cyclohexane at room temperature as shown in Fig. 4. The observed band is separated by about 1000  $\text{cm}^{-1}$  from the 0-0 band of the phosphorescence spectrum. These observations suggest that the lowest triplet state of this molecule is a  $^3(\pi, \pi^*)$  state and a  $^3(n, \pi^*)$  state is located about 1000  $\text{cm}^{-1}$  above the phosphorescent  $^3(\pi, \pi^*)$  state. These assignments of the states are consistent with the relatively short  $\pi \leftarrow \pi^*$  phosphorescence lifetime and the complicated vibronic structure of the phosphorescence spectrum. The strong intensities of the 0-0 and totally symmetric  $\nu_5$  and  $\nu_2$  bands in the short lifetime phosphorescence spectrum indicate that the lowest  $^3(\pi, \pi^*)$  state is strongly coupled with the  $^1B_1(n, \pi^*)$  state through the first order spin-orbit interaction. This means that the short lifetime phosphorescence arises from the  $B_1$  triplet sublevel. Observations of the out-of-plane  $b_1$  and  $a_2$  bands with medium intensity in the short lifetime phosphorescence and the remarkable intensification of the  $a_2$  vibronic bands relative to the intensity of the 0-0 band in the middle lifetime phosphorescence indicate that the phosphorescent  $^3(\pi, \pi^*)$  state is vibronically coupled with the closely located  $^3(n, \pi^*)$  states as suggested by Scharf and Leismann.<sup>2)</sup>

*Near Ultraviolet Absorption Spectrum.*

The near

ultraviolet absorption spectra observed in cyclohexane and the thin film prepared by sublimation at room temperature and 77 K, respectively, are shown in Fig. 4. The absorption observed in the 290–230 nm region with  $\epsilon \approx 7000$  in cyclohexane loses the intensity in the thin film spectrum. We observed the infrared spectrum of the thin film sample with the unpolarized light. The  $b_2$  and  $b_1$  vibrational bands were observed with strong intensity, while the  $a_1$  band with very weak intensity. This observation clearly indicates that the 290–230 nm absorption should be ascribed to the  $^1A_1(\pi, \pi^*) \leftarrow ^1A_1$  transition.

The absorption observed in the 350–300 nm region with  $\epsilon \approx 25$  in cyclohexane, which was ascribed to the  $n \rightarrow \pi^*$  transition by Scharf and Leismann,<sup>2)</sup> shifts toward the blue side in the thin film. Generally the absorption observed in the solid at low temperature shows the red shift and hence two absorption systems are expected to locate in this region. We observed the polarized near ultraviolet absorption spectrum of the single crystal grown between two quartz plates and the result is shown in Fig. 4. The notations of the  $\parallel$  and  $\perp$  spectra are the same as those given in the polarized infrared spectrum of the single crystal grown between two KRS-5 plates. The observation indicates that the polarization of the 350–325 nm absorption is clearly different from that of the 325–300 nm absorption. By analogy with the polarization behaviors of the infrared bands, the former absorption could be ascribed to the forbidden  $^1A_2(n, \pi^*) \leftarrow ^1A_1$  transition perturbed by the  $^1A_1(\pi, \pi^*) \leftarrow ^1A_1$  transition and the latter to the  $^1B_1(n, \pi^*) \leftarrow ^1A_1$  transition.

The phosphorescence excitation spectrum observed in cyclohexane at 77 K gives well resolved vibrational structure as shown in Fig. 4. The longest wavelength and very weak band at 355.0 nm was taken as the 0-0 band of the  $^1A_2(n, \pi^*) \leftarrow ^1A_1$  absorption, which may appear in the spectrum by the crystal field dis-

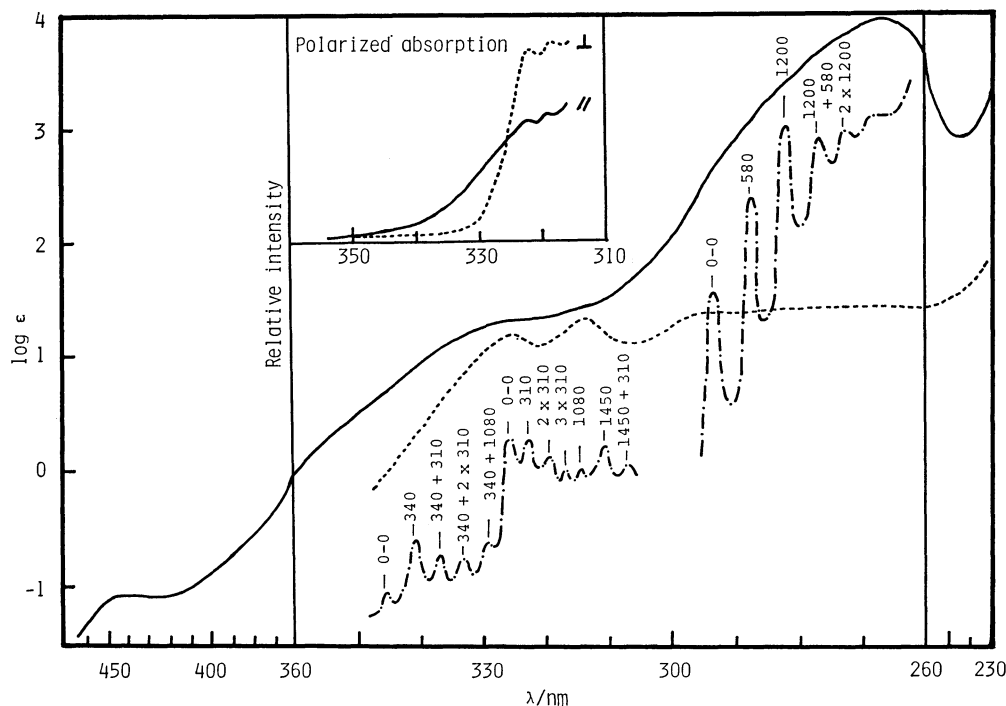


Fig. 4. Near ultraviolet absorption and phosphorescence excitation spectra of dichloromaleic anhydride. —: Absorption spectrum in cyclohexane at room temperature, ----: absorption spectrum in the thin film at 77 K, - · - · -: phosphorescence excitation spectrum in cyclohexane at 77 K. Polarization behavior of the 350—315 nm absorption region is shown in the upper part of the figure. The absorption spectrum in cyclohexane was plotted against  $\log \epsilon$ , while the other spectra were against relative intensity.

tortion. A strong band separated by  $340\text{ cm}^{-1}$  from the 0-0 band was ascribed to the perturbing vibration of the  $a_2$  species. The frequency of  $340\text{ cm}^{-1}$  was assigned to the upper state frequency of the C=O wagging ( $\nu_{17}$ ) vibration. This assignment would be reasonable because the C=O wagging vibration could be expected to be most effective for the vibronic coupling between the  $(n, \pi^*)$  and  $(\pi, \pi^*)$  states. Band intervals of  $310$  and  $1080\text{ cm}^{-1}$  were observed and these were assigned to the upper state frequencies of the C=O bending ( $\nu_7$ ) and C—O stretching ( $\nu_3$ ) vibrations of the  $a_1$  species, respectively.

A strong band at  $325.7\text{ nm}$  was taken as the 0-0 band of the  ${}^1B_1(n, \pi^*) \leftarrow {}^1A_1$  absorption. The upper state frequencies of the  $\nu_7$  and  $\nu_3$  vibrations were also observed in this absorption. A strong band separated by  $1450\text{ cm}^{-1}$  from the 0-0 band was ascribed to the upper state C=O stretching ( $\nu_1$ ) vibration of the  $a_1$  species.

A strong band at  $293.2\text{ nm}$  was taken as the 0-0 band of the  ${}^1A_1(\pi, \pi^*) \leftarrow {}^1A_1$  absorption. Band separations of  $580$  and  $1200\text{ cm}^{-1}$  were observed and these were assigned to the upper state frequencies of the ring deformation ( $\nu_5$ ) and C=C stretching ( $\nu_2$ ) vibrations of the  $a_1$  species, respectively. These vibrations were observed quite strongly in the  ${}^3(\pi, \pi^*) \rightarrow$

${}^1A_1$  phosphorescence spectrum as described above.

The CNDO-MO calculation suggests that the two  $n$  orbitals on the O atoms of the C=O bonds couple with each other through the C—O bonds and hence the  $n \rightarrow \pi^*$  transition gives rise to changes of the C=O and also C—O bond characters. Therefore, the observations of the C=O bending, C—O stretching, and C=O stretching vibrations in the  ${}^1A_2(n, \pi^*) \leftarrow {}^1A_1$  and  ${}^1B_1(n, \pi^*) \leftarrow {}^1A_1$  excitation spectra could be reasonably understood.

## References

- 1) A. Rogstad, P. Klaboe, B. N. Cyvin, S. J. Cyvin, and D. H. Christensen, *Spectrochim. Acta, Part A*, **28**, 111 (1972).
- 2) H.-D. Scharf and H. Leismann, *Z. Naturforsch., B*, **28**, 662 (1973).
- 3) Y. Ishibashi, R. Shimada, and H. Shimada, *Bull. Chem. Soc. Jpn.*, **55**, 2765 (1982).
- 4) S. Kizuki, Y. Ishibashi, H. Shimada, and R. Shimada, *Mem. Fac. Sci. Kyushu Univ. Ser. C*, **13**, 7 (1981).
- 5) Y. Urabe, T. Watanabe, Y. Ishibashi, H. Shimada, and R. Shimada, *Mem. Fac. Sci. Kyushu Univ. Ser. C*, **13**, 1 (1981).
- 6) R. L. Hilderbrandt and E. M. A. Peixoto, *J. Mol. Struct.*, **12**, 31 (1972).